Adsorption of Benzene and Methyl-Substituted Benzenes at the Vapor/Water Interface. 2. Single-Component VHOC Adsorption

Robert G. Bruant, Jr. and Martha H. Conklin*

Department of Hydrology and Water Resources, The University of Arizona, P.O. Box 210011, Harshbarger Building 11, Tucson, Arizona 85721-0011

Received: August 10, 2000; In Final Form: December 12, 2000

Equilibrium isothermal relationships between aqueous solution surface tension and vapor-phase solute pressure of individual volatile hydrophobic organic compounds (VHOCs) (benzene, methylbenzene, 1,2-dimethylbenzene, 1,3-dimethylbenzene, 1,4-dimethylbenzene, and 1,3,5-trimethylbenzene) were measured employing a dynamic adsorption method, axisymmetric drop shape analysis-profile (ADSA-P), and gas chromatographic analysis. Systems were analyzed at atmospheric pressure in duplicate at 285.2, 291.2, 297.2, 303.2, and 315.2 K, for vapor-phase VHOC pressures up to saturated vapor pressure. Developed isotherms were fit with a mathematical form combining a nonideal two-dimensional equation of state and the Gibbs relative interface excess equation. Derived functions were used to quantify vapor/water relative interface solute excess, interface-phase activity coefficients, and ideal standard molar Gibbs free energy, enthalpy, and entropy changes of adsorption. Results indicate that molecular size dictates adsorption among the compounds considered, with generally increased interface excess and isotherm nonideality as molecular size increased. Calculated values for ideal free energy change of adsorption (at infinite dilution) were linear as a function of temperature and evenly spaced as a function of methyl substitution (approximately $2-3 \times 10^3$ J mol^{-1} more negative for each methyl substitution). Calculated values for enthalpy change were less negative than the corresponding values of liquefaction, suggesting specific interactions between solutes and interface-phase water molecules. Entropy changes, more negative than predicted for the loss of one translational degree of freedom, further support this conclusion.

Introduction

Determining distribution and retention mechanisms for contaminants in environmental systems is necessary for addressing exposure risk, persistence, and possible means of compound removal. Of particular environmental concern are volatile hydrophobic organic compounds (VHOCs), derived from petroleum products and industrial solvents. Discharged both accidentally and deliberately, these compounds have become ubiquitous contaminants, posing health risks due to their toxicity and potential carcinogenicity. In systems containing large vapor/water interfacial area to bulk volume ratios (e.g., unsaturated soil matrixes, atmospheric fog, and rain droplets), the vapor/water interface has been identified as a meaningful site for VHOC retention.[1−6] Nevertheless, due to difficulties in containing and analyzing these weakly soluble volatile compounds, a paucity of sound experimental data and associated analysis exists regarding adsorption, both in terms of magnitude and mechanism, at this important environmental interface.

Recently, we detailed a new measurement technique combining axisymmetric drop shape analysis-profile (ADSA-P)[7,8] (for surface tension measurement), gas chromatographic analysis (for vapor-phase VHOC (i.e., solute) pressure measurement), and a dynamic adsorption protocol to experimentally determine aqueous solution surface tension (converted to surface pressure for analysis and presentation clarity) as a function of vapor-phase pressure isotherms for analysis of benzene and trichloroethene adsorption at the vapor/water interface.[9,10] The experimental system and approach eliminated potential bias of a three-phase boundary during surface tension measurement, allowed rigorous measurement of vapor-phase VHOC pressures, especially in the dilute limit, and provided definition of experimental isothermal relationships consisting of tens to hundreds of points in just several hours.

The current study provides further measurement and analysis of benzene and methyl-substituted benzene (methylbenzene (MB), 1,2-dimethylbenzene (12DMB), 1,3-dimethylbenzene (13DMB), 1,4-dimethylbenzene (14DMB), and 1,3,5-trimethylbenzene (135TMB)) adsorption at the vapor/water interface. To address adsorption magnitude and solute−solute interactions at finite VHOC concentrations, relative interface excess of the volatile solute components and two-dimensional interface-phase activity coefficients are calculated from measured aqueous solution surface tension (pressure) isotherms. At limiting solute concentrations, where solute−solute interactions are negligible, ideal standard molar Gibbs free energy, enthalpy, and entropy changes of adsorption are derived to consider interactions between solutes and interface water molecules. The overall goal of this research is to address the systematic effect of both the degree and position of methyl substitution on vapor/water interface adsorption over a 30 K temperature range. The work allows consideration of compounds/temperatures not previously examined, critique of previous (though limited) measurements of aromatic hydrocarbon adsorption, and evaluation of predictive approaches for defining vapor/water interface adsorption parameters.

Theory

Thermodynamics. For single-component volatile solute adsorption at the vapor/water interface at atmospheric pressure,

* Corresponding author. E-mail: martha@hwr.arizona.edu. Telephone: 520-621-5829. Fax: 520-621-1422.

10.1021/jp0029156 CCC: $22.00
Published on Web 02/05/2002

constant temperature, and phase equilibrium, the Gibbs relative interface excess equation is given as[11]

$$d\pi = \Gamma\, d\mu^{V} \quad (1)$$

where π is the actual (measured) aqueous solution surface pressure (surface tension of solute-free water less measured aqueous solution surface tension) [N m^{-1}], Γ is the relative interface excess of the volatile solute component per unit area (with the interface excess of water (solvent) equal to zero and neglecting air) [mol m^{-2}], and μ^{V} is the vapor-phase (V) chemical potential of the solute [J mol^{-1}] defined as

$$\mu^{V} = \mu^{V,0} + RT\ln(f^{V}/f^{V,0}) = \mu^{V,0} + RT\ln(p^{V}\phi^{V}/f^{V,0}) \quad (2)$$

where $\mu^{V,0}$ is the standard-state vapor-phase solute chemical potential [J mol^{-1}], R is the molar gas constant [J mol^{-1} K^{-1}], T is the absolute temperature [K], f^{V} is the three-dimensional vapor-phase solute fugacity [Pa], $f^{V,0}$ is the three-dimensional standard-state vapor-phase solute fugacity [Pa] ($\equiv 1.01325 \times 10^{5}$ Pa), p^{V} is the vapor-phase solute pressure [Pa], and ϕ^{V} is the vapor-phase activity coefficient defined on an *un*symmetric basis (i.e., $\phi^{V} \rightarrow 1$ as $p^{V} \rightarrow 0$) [unitless].[12-14] Assuming perfect vapor-phase behavior at atmospheric pressure (i.e., $\phi^{V} \approx 1$), differentiation of eq 2 and substitution into eq 1 gives a form of the Gibbs relative interface excess equation for single volatile solute adsorption at the vapor/water interface in terms of vapor-phase solute pressure:

$$d\pi = \Gamma kT\, d\ln p^{V} \quad (3)$$

To quantify equilibrium thermodynamics of solute adsorption, the interface-phase (I) solute chemical potential μ^{I} [J mol^{-1}] is defined in a manner similar to that in eq 2:[12,13,15-17]

$$\mu^{I} = \mu^{I,0} + kT\ln(f^{I}/f^{I,0}) = \mu^{I,0} + kT\ln(\pi^{ideal}\gamma^{I}/f^{I,0}) \quad (4)$$

where $\mu^{I,0}$ is the standard-state interface-phase solute chemical potential [J mol^{-1}], f^{I} is the two-dimensional interface-phase solute fugacity ($\equiv\pi$) [N m^{-1}], $f^{I,0}$ is the two-dimensional standard-state interface-phase solute fugacity [N m^{-1}] ($\equiv 6.07950 \times 10^{-5}$ N m^{-1}),[17] π^{ideal} is the ideal aqueous solution surface pressure (i.e., no interface solute−solute interactions) [N m^{-1}], and γ^{I} is the two-dimensional interface-phase activity coefficient defined on an unsymmetric basis (i.e., $\gamma^{I} \rightarrow 1$ as $\pi^{ideal} \rightarrow 0$) [unitless]. The standard Gibbs free energy change of solute adsorption $\Delta_{ads}g^{0}_{(V\rightarrow I)}$ [J mol^{-1}] is then derived from combination of eqs 2 and 4 at phase equilibrium (again assuming perfect vapor-phase solute behavior and using the common notation of actual aqueous solution surface pressure for definition of interface-phase solute fugacity):[15,16,18]

$$\Delta_{ads}g^{0}_{(V\rightarrow I)} = -RT\ln(\pi^{ideal}\gamma^{I}/\tau p^{V}) = -RT\ln(\pi/\tau p^{V}) \quad (5)$$

where τ is the Kemball−Rideal interface thickness ($\equiv f^{I,0}/f^{V,0} = 6 \times 10^{-10}$ m).[17] This defines the change in the standard-state chemical potential for a volatile solute transferred from the vapor phase to the vapor/water interface (i.e., V→I). Using established thermodynamic relationships, the equilibrium standard molar enthalpy change $\Delta_{ads}h^{0}_{(V\rightarrow I)}$ [J mol^{-1}] and equilibrium standard molar entropy change $\Delta_{ads}s^{0}_{(V\rightarrow I)}$ [J mol^{-1} K^{-1}] can then be quantified:[13,19]

$$\Delta_{ads}h^{0}_{(V\rightarrow I)} = [\partial(\Delta_{ads}g^{0}_{(V\rightarrow I)}/T)/\partial(1/T)]_{\pi} \quad (6)$$

and

$$\Delta_{ads}s^{0}_{(V\rightarrow I)} = -[\partial(\Delta_{ads}g^{0}_{(V\rightarrow I)})/\partial T]_{\pi} \quad (7)$$

Data Interpolation. To mathematically define the relationship between aqueous solution surface pressure and vapor-phase VHOC pressure from experimentally derived isothermal relationships, the data was fit using a combined form of a nonideal two-dimensional equation of state and the Gibbs relative interface excess equation. The goal was to define a functional form for consistent mathematical interpretation of the data. The nonideal equation of state is defined as

$$\pi(a - a^{0}) = RT \quad (8)$$

where a is the molar area projection [m^{2} mol^{-1}] and a^{0} is an empirical fitting constant [m^{2} mol^{-1}].[12,17,20-22] Combining with eq 3 (where $a = \Gamma^{-1}$) and integrating gives the resulting nonideal equation of surface pressure used in this study:

$$p^{V} = \pi \exp(\pi a^{0}/RT + c) \quad (9)$$

where c is an integration constant [unitless]. The given equation was fit to the experimental data using a nonlinear least-squares regression routine to define values for a^{0} and c. To approximate the relative interface excess for each measurement of surface tension (pressure), eq 8 was rearranged, incorporating the interpolated a^{0} values from eq 9:

$$\Gamma = (RT/\pi + a^{0})^{-1} \quad (10)$$

To quantify ideal aqueous solution surface pressure as a function of vapor-phase solute pressure, for both determination of ideal thermodynamic parameters of adsorption (at limiting surface pressures) and two-dimensional interface-phase activity coefficients at finite surface pressures, a similar expression to eq 9 was defined from the ideal two-dimensional equation of state:

$$\pi^{ideal}a = RT \quad (11)$$

Combining eq 11 with eq 3 and integrating gives the ideal equation of surface pressure:

$$p^{V} = \pi^{ideal}\exp(c) \quad (12)$$

where c is determined from fit of eq 9 to the experimental data. Using eqs 5−7 and 12 allows direct determination of the ideal standard molar Gibbs free energy change (eq 13), ideal standard molar enthalpy change (eq 14), and ideal standard molar entropy change (eq 15) of adsorption from the interpolated parameters of eq 9:

$$\Delta_{ads}g^{0,ideal}_{(V\rightarrow I)} = -RT[\ln(1/\tau) - c] \quad (13)$$

$$\Delta_{ads}h^{0,ideal}_{(V\rightarrow I)} = R[\partial c/\partial(1/T)]_{\pi\rightarrow 0} \quad (14)$$

and

$$\Delta_{ads}s^{0,ideal}_{(V\rightarrow I)} = \{R\ln(1/\tau) - R[\partial(Tc)/\partial T]\}_{\pi\rightarrow 0} \quad (15)$$

The interface-phase activity coefficient can be derived from combination of eqs 9 and 12:

$$\gamma^{I} = \exp(-\pi a^{0}/RT) \quad (16)$$

which provides a measure of deviation from ideal adsorption at finite surface pressures.

Materials and Methods

Chemicals. Benzene (C_6H_6, ≥99.5%), methylbenzene ($[CH_3]$-C_6H_5, ≥99.5%), 1,2-dimethylbenzene (1,2-$[CH_3]_2C_6H_4$, ≥99%), 1,3-dimethylbenzene (1,3-$[CH_3]_2C_6H_4$, ≥99%), 1,4-dimethylbenzene (1,4-$[CH_3]_2C_6H_4$, ≥99%), and 1,3,5-trimethylbenzene (1,3,5-$[CH_3]_3C_6H_3$, ≥99%) were purchased from Fluka Chemical (Ronkonkoma, NY) and used without further refinement. Water from a Millipore deionization system was distilled at atmospheric pressure in a potassium permanganate/sodium hydroxide solution followed by all-water distillation; liquids were assumed to have equilibrium concentrations of atmospheric air.

Experimental System. Detail of the experimental system is presented elsewhere,[25] and only a brief summary is currently given. Aqueous solution surface tension measurements were made at atmospheric pressure using pendant drop tensiometry. Drops were formed from a Teflon capillary inside a gastight 316-gauge stainless steel environmental cell. The cell temperature was regulated (±0.2 K) by an exterior brass jacket attached to thermoelectric heating/cooling devices; Styrofoam was used for insulation. The cell and surrounding thermal regulation system were mounted on an isolation bench for vibration control. Pendant drops were illuminated by a diffuse halogen light source and imaged using a charge-coupled device (CCD) video camera. Recorded images were analyzed using axisymmetric drop shape analysis-profile (ADSA-P) software acquired from Applied Surface Thermodynamics Research Associates (Toronto, Ontario).

Gas-washing bottles (Chemglass, Vineland, NJ) were used to contact advecting air with both liquid water and liquid organic phases for vapor delivery to the environmental cell. Mass flow controllers (Hasting Instruments, Hampton, VA) regulated volumetric flow. A 1.5×10^{-8} m^3 electronically actuated sample loop was attached at the immediate environmental cell outlet for automated sampling of the vapor-phase. Samples were transferred directly through fused silica tubing to a Varian 3600CX gas chromatograph (GC) with flame ionization detector (FID) for determination of vapor-phase solute pressures.

Measurement Protocol. Experiments were initiated by forming a VHOC-free pendant water drop in contact with advecting humidified air. After thermal and mechanical equilibration of the water drop, VHOC delivery was switched to the cell. Simultaneously, automated image acquisition and sample injection to the GC were started, with measurements made at 120 s intervals. The air/vapor flow rates for isotherm measurements were approximately 3×10^{-8} m^3 s^{-1} (STP), sufficient to deliver a well dispersed solute front (i.e., slowly increasing vapor-phase VHOC pressure) without appreciable physical disturbance of the water drop. Mean aqueous solution surface tensions (arithmetic mean calculated from 30 replicate selections and analyses of 20 coordinates along each drop profile) and GC peak areas were continuously monitored to determine when minimum and maximum values were reached, respectively (always less than 3.6×10^4 s).

Aqueous solution surface tension (pressure) measurements were matched to vapor-phase VHOC pressures (assumed to represent the average vapor-phase solute pressure for the cell interior at the time of sampling) for each analysis time to generate individual isotherm coordinates. Adsorption was rapid (≤10 s to equilibrium).[9,10] Complete isotherms (i.e., final vapor-phase solute pressures p^V_{max} approximately equal to saturated vapor pressure for the system temperature p^V_{sat}) were measured in duplicate at cell temperatures of 287.2, 291.2, and 297.2 K for all compounds investigated. Isotherms were also measured in duplicate at 303.2 and 315.2 K, but maximum vapor-phase VHOC pressures were limited ($p^V_{max} < p^V_{sat}$) by ambient room temperatures (<298 K). Measurements at 315.2 K of 135TMB were not included due to insufficient isotherm resolution (measured maximum surface tension change not significantly different than lumped surface tension measurement accuracy ($\pm 2 \times 10^{-4}$ N m^{-1}; derived from replicate measurements of clean water and clean benzene liquid phases)).

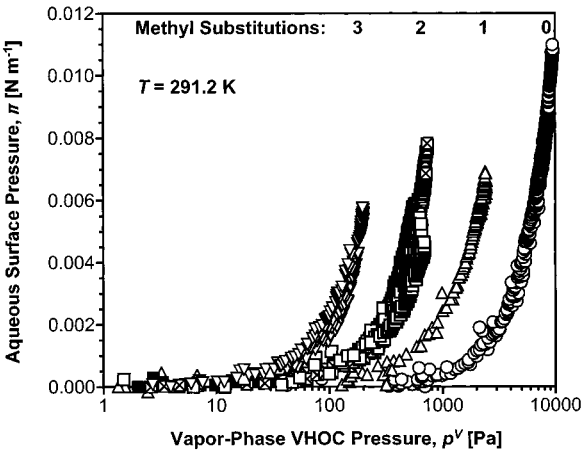

Figure 1. Measured aqueous solution surface pressure π as a function of vapor-phase VHOC pressure p^V isotherms at 291.2 K: benzene (circle), MB (upright triangle), 12DMB (solid square), 13DMB (square with "×" inside), 14DMB (open square), and 135TMB (upside down triangle). Methyl substitutions: benzene (0); MB (1); 12DMB, 13DMB, 14DMB (2); 135TMB (3).

Results

Measured aqueous solution surface pressure as a function of vapor-phase VHOC pressure isotherms for benzene, MB, 12DMB, 13DMB, 14DMB, and 135TMB are given in Figure 1 for the replicate 291.2 K experiments. Plots are presented linearly with respect to the aqueous solution surface pressure axis and logarithmically with respect to the vapor-phase VHOC pressure axis. Distinct and relatively equivalent separation between measured profiles is evident with respect to the degree of methyl substitution (0 ≡ benzene; 1 ≡ MB; 2 ≡ 12DMB, 13DMB, and 14DMB; and 3 ≡ 135TMB), but with little discernible difference related to the position of substitution for the dimethylbenzene isomers. The VHOC pressure necessary to induce an equivalent change in surface tension decreases by a factor of approximately 3−3.5 for each methyl group added, similar to Traube's rule for a homologous series of alkane chains (approximately a factor of 3 decrease in concentration for each methylene addition).[19] Maximum deviations between replicate aqueous solution surface pressure measurements for a given vapor-phase solute pressure are $\sim 1 \times 10^{-3}$ N m^{-1} (near saturated vapor pressure), however significantly less difference is standard. Subsequent adsorption parameters are calculated from combination of replicate experimental data (i.e., composite), with error estimates derived from the maximum deviation to individual replicates (vide infra).

The temperature dependence of the measured aqueous solution surface pressure isotherms is illustrated in Figure 2 for 13DMB. As the system temperature decreases, there is a concurrent increase in the surface pressure for a given vapor-phase VHOC pressure. All complete isotherms exhibit a general

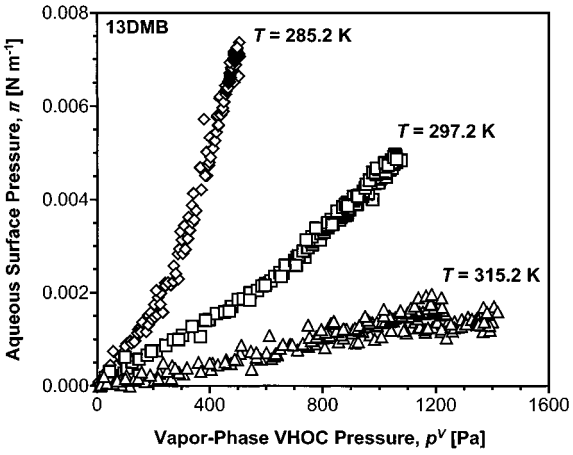

Figure 2. Measured aqueous solution surface pressure π as a function of vapor-phase 13DMB pressure p^V isotherms: 285.2 K (diamond), 297.2 K (square), and 315.2 K (triangle).

TABLE 1: Nonideal Equation of Surface Pressure (Equation 3) Parameters for Composite Measured Aqueous Solution Surface Pressure versus Bulk Vapor-Phase VHOC Pressure Isotherms

solute	T [K]	$p^V_{max}\,p^V_{sat}{}^{-1}$	$a^0 \times -10^{-5}$ [m^2 mol^{-1}]	$c \times 10^{-1}$ [unitless]	R^2 [a]
B[b]	285.2	1.06	0.903	1.38	0.993
	291.2	1.05	1.28	1.43	0.994
	297.2	0.998	1.64	1.46	0.997
	303.2	0.797	0.711	1.47	0.988
	315.2	0.536	2.09	1.55	0.945
MB	285.2	0.926	1.40	1.27	0.987
	291.2	0.944	0.820	1.30	0.993
	297.2	0.881	1.09	1.33	0.995
	303.2	0.839	1.51	1.38	0.972
	315.2	0.567	−0.439	1.45	0.963
12DMB	285.2	1.05	2.62	1.17	0.992
	291.2	1.00	2.23	1.20	0.993
	297.2	0.999	2.47	1.24	0.992
	303.2	0.770	0.646	1.25	0.990
	315.2	0.424	4.24	1.37	0.828
13DMB	285.2	0.990	2.30	1.18	0.990
	291.2	1.00	2.09	1.21	0.992
	297.2	1.01	2.00	1.27	0.995
	303.2	0.817	−1.28	1.28	0.993
	315.2	0.502	6.31	1.39	0.872
14DMB	285.2	0.951	2.31	1.18	0.993
	291.2	0.893	2.12	1.22	0.951
	297.2	0.933	2.44	1.26	0.955
	303.2	0.781	1.74	1.28	0.980
	315.2	0.628	0.667	1.38	0.922
135TMB	285.2	0.969	3.41	1.09	0.985
	291.2	0.969	2.29	1.10	0.972
	297.2	0.976	2.30	1.15	0.977
	303.2	0.782	2.08	1.23	0.882

[a] Coefficient of determination. [b] B indicates benzene.

monotonic increase in surface pressure with increasing vapor-phase VHOC pressure, convex to the surface pressure axis. There is no indication from any of the profiles that a limiting surface pressure is reached or an interface-phase phase change occurs for the solutes. Measurements made at 303.2 K (not shown) and 315.2 K do not exhibit the same degree of curvature as isotherms derived at the lower temperatures, assumed due to the fact that the highest measured vapor-phase VHOC pressures were only a fraction of saturated vapor pressure ($p^V_{max}\,p^V_{sat}{}^{-1}$, Table 1) and the corresponding high noise-to-signal ratios for these low vapor-phase solute pressure/surface pressure measurements.

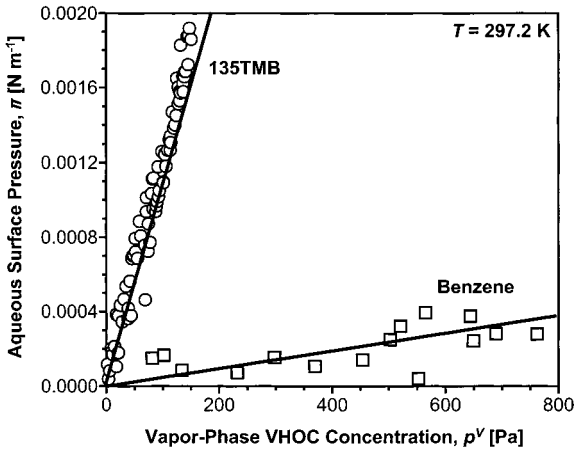

Figure 3. Comparison of measured aqueous solution surface pressure π as a function of vapor-phase benzene (square) and 135TMB (circle) pressure p^V isotherms to interpolations using the ideal equation of surface pressure (eq 12, lines) at 297.2 K.

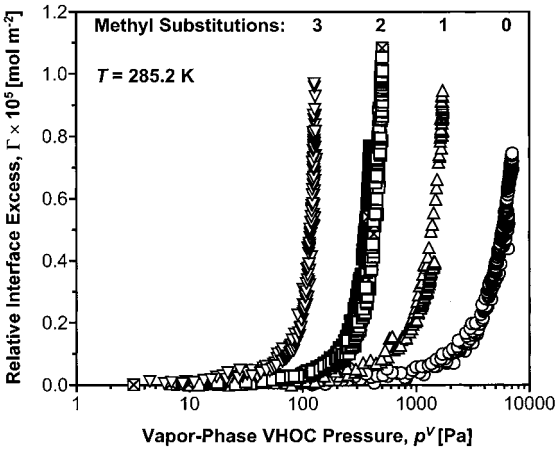

Figure 4. Relative VHOC interface excess, Γ, as a function of vapor-phase VHOC pressure, p^V, isotherms at 285.2 K: benzene (open circle), MB (upright triangle), 12DMB (solid square), 13DMB (square with "×" inside), 14DMB (open square), 135TMB (upside down triangle). Methyl substitutions: benzene (0); MB (1); 12DMB, 13DMB, 14DMB (2); and 135TMB (3).

Discussion

Data and Interpolation. Results of aqueous solution surface pressure isotherm curve fitting for the composite replicate experiments using eq 9 are provided in Table 1. The coefficients of determination, in addition to visual inspection, indicate that eq 9 empirically provides an accurate representation of the experimental data, especially when applied to measurements of near-complete isotherms (i.e., $p^V_{max}\,p^V_{sat}{}^{-1} \geq 0.9$). Additionally good representation of the data is achieved in the low surface pressure/low vapor-phase pressure region using eq 12 (cf. Figure 3). Reduced coefficients of determination for higher temperature experiments were assumed to be a function of the increased relative error of measurements made in the lower aqueous solution surface pressure/vapor-phase VHOC pressure region.

Relative Interface Excess. Relative VHOC interface excess as a function of vapor-phase VHOC pressure isotherms were calculated from the composite surface pressure isotherms using eq 10 and the derived a^0 values from eq 9 (Table 1). Results as a function of solute type are presented semilogarithmically in Figure 4 for 285.2 K. As noted previously for the surface pressure isotherms, there is a constant separation between relative interface excess isotherms as a function of degree of methyl substitution, with increased adsorption associated with

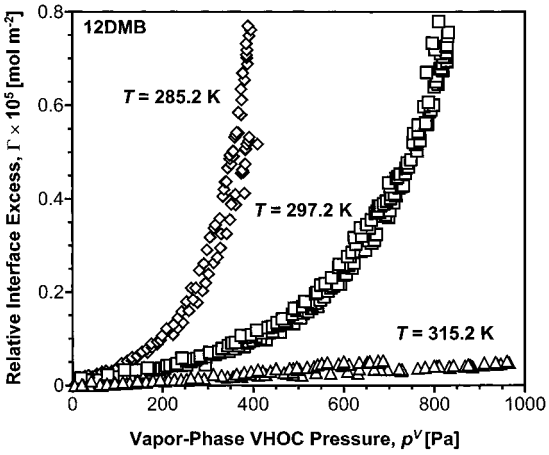

Figure 5. Relative 12DMB interface excess Γ as a function of vapor-phase 12DMB pressure p^V isotherms: 285.2 K (diamond), 297.2 K (square), and 315.2 K (triangle).

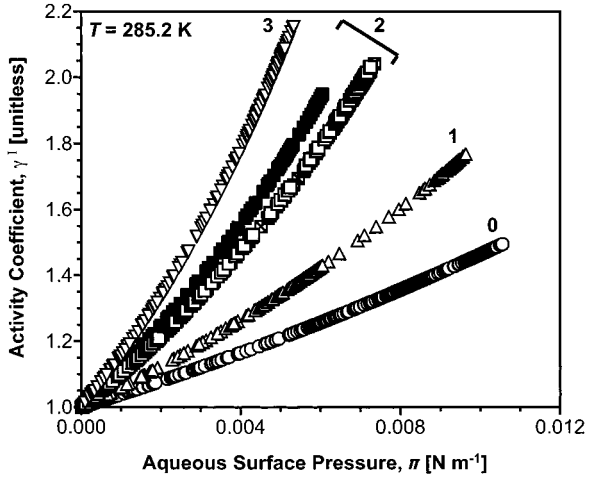

Figure 6. Interface-phase activity coefficients, γ^I, as a function of measured aqueous solution surface pressure, π, at 285.2 K: benzene (open circle), MB (upright triangle), 12DMB (solid square), 13DMB (square with "×" inside), 14DMB (open square), and 135TMB (upside down triangle). Numbers indicate of methyl substitutions: Benzene (0); MB (1); 12DMB, 13DMB, 14DMB (2); and 135TMB (3).

greater substitution. Maximum relative interface VHOC excess values were on the order of 10^{-5} mol m^{-2} for all systems considered. Typical temperature dependence of the excess calculations is provided in Figure 5 for 12DMB. For a given vapor-phase solute pressure, interface excess increases as temperature decreases. Relative interface excess isotherms calculated from lower temperature experiments (e.g., 285.2 and 297.2 K) exhibit significant nonlinearly, especially at high vapor-phase VHOC pressures, while such behavior is generally absent from the higher temperature experimental results (e.g. 315.2 K).

Finite Adsorption Activity Coefficients. Calculation of the interface-phase activity coefficients γ^I (eqs 4 and 16) were used to quantify the magnitude and controlling factors of interface-adsorption nonideality. Activity coefficients were calculated only for near complete composite surface pressure isotherms (i.e., at 285.2, 291.2, and 297.2 K). Maximum interface-phase activity coefficients ranged from 1.2 to 2.2 for the compounds and temperatures considered. Figure 6 provides illustration of the activity coefficients as a function of measured aqueous solution surface pressure for the 285.2 K experiments. For the presented results, it is apparent that the activity coefficients increase as the number of benzene substitutions increase. The trend, however, is not as apparent for the other temperatures considered, especially with regard MB (which has a significantly smaller activity correction at 291.2 and 297.2 K than benzene). Further definition of complete surface pressure isotherms over a broader temperature range is necessary to better constrain structure and temperature dependence of interface-phase activity coefficients.

Ideal Gibbs Free Energy Change. The ideal standard molar Gibbs free energy changes of adsorption $\Delta_{ads}g^{0,ideal}_{(V\rightarrow I)}$ (eq 13) as a function of temperature are presented in Table 2 and Figure 7. Error bars represent the maximum difference between values calculated from composite replicate isotherms and the individual replicates, and suggest good reproducibility. All calculated ideal free energy changes of adsorption are negative, indicating a favorable reduction due to transfer of the VHOCs from the vapor-phase to the vapor/water interface at infinite dilution. Temperature dependence, in general, is linear, with minor scatter about the provided linear fits to the composite values.

The degree of methyl substitution significantly influences the ideal free energy changes of adsorption, with more negative values (i.e., greater interface affinity) corresponding to increased solute substitution at a given temperature. The position of substitution for the dimethylbenzene isomers (DMB) only imparts subtle differences in the calculated values, especially in comparison to the contribution by methyl addition. Combining the results for the dimethylbenzene isomers, the average changes (arithmetic mean of the five temperatures considered for each solute) between benzene and MB, MB and DMB, and DMB and 135TMB composite values are 2.8×10^3 , 2.2×10^3, and 2.7×10^3 J mol^{-1}, respectively. This consistent variation in free energy change with regard to methyl substitution is again analogous (and roughly equivalent) to the Traube's rule relationship defined for methylene addition to *n*-alkanes.[19]

Comparison to the previous calculations of ideal standard molar Gibbs free energy changes of adsorption available in the literature reveals variable agreement. Blank and Ottewill[23] measured surface pressure versus vapor-phase solute pressure isotherms for benzene (273.2 K, 280.7, and 288.2 K), MB (278.2 and 288.2 K), and 12DMB (288.2 K) using a torsion balance with mica/platinum plates; free energy change results are included in Figure 7. Agreement is satisfactory for the benzene experiments, but less so for MB (our current composite calculations $\sim 1.4 \times 10^3$ J mol^{-1} more negative) and 12DMB (our current composite calculations $\sim 3.8 \times 10^3$ J mol^{-1} more negative). However, Ottewill (cf. ref 24) questioned the quality of their results due to insufficient resolution of isotherm shape at low surface pressures (the small difference between MB and 12DMB free energy changes is suspect (cf. Figure 7)), which may help explain the observed discrepancy with our current values. Hauxwell and Ottewill[24] again measured the adsorption of MB at the vapor/water interface using principally the same technique. Calculated ideal standard molar free energy change results are given also in Figure 7 and visually are only slightly different from previous values.[23] On the other hand, Karger and co-workers,[25−27] using a chromatographic retention method to derive adsorption data, calculated ideal free energy changes at 285.7 K (the only temperature reported) for benzene (-1.8×10^4 J mol^{-1}) and MB (-2.0×10^4 J mol^{-1}), which correspond well with the current composite calculations at 285.2 K of -1.76×10^4 J mol^{-1} and -2.03×10^4 J mol^{-1}, respectively.

Current results were used to test the utility of the semi-empirical equation for prediction of $\Delta_{ads}g^{0,ideal}_{(V\rightarrow I)}$ given by Valsaraj:[6,28]

$$\Delta_{ads}g^{0,ideal}_{(V\rightarrow I)} = \Delta_{henry}g^{0,ideal}_{(V\rightarrow W)} + (A_m/4)[2\phi(\sigma_{IV}\sigma_{WV})^{1/2} - 2\sigma_{WV}] \quad (17)$$

TABLE 2: Calculated Composite Ideal Standard Molar Gibbs Free Energy, Enthalpy, and Entropy Changes of Adsorption and Comparison with Energetics of Vapor/Water Transfer (Henry's Law)

solute	T [K]	$\Delta_{ads}g^{0,ideal}_{(V\rightarrow I)} \times -10^{-4}$ [J mol^{-1}]	$\Delta_{ads}h^{0,ideal}_{(V\rightarrow I)} \times -10^{-4}$ [J mol^{-1}][a]	$\Delta_{ads}s^{0,ideal}_{(V\rightarrow I)} \times -10^{-1}$ [J mol^{-1} K^{-1}][a]	$\Delta_{ads}g^{0,ideal}_{(V\rightarrow I)} \times -10^{-4}$ [J mol^{-1}][b]	$\Delta_{henry}g^{0,ideal}_{(V\rightarrow W)} \times -10^{-3}$ [J mol^{-1}][c]	$\Delta_{henry}h^{0,ideal}_{(V\rightarrow W)} \times -10^{-4}$ [J mol^{-1}][a]
B[d]	285.2	1.76	4.10	8.3	1.61	4.43	2.20
	291.2	1.69			1.59	4.06	
	297.2	1.64			1.58	3.69	
	303.2	1.64			1.56	3.31	
	315.2	1.49			1.53	2.57	
MB	285.2	2.03	4.71	9.4	1.88	3.96	2.04
	291.2	1.99			1.86	3.62	
	297.2	1.97			1.84	3.27	
	303.2	1.86			1.82	2.92	
	315.2	1.76			1.79	2.23	
12DMB	285.2	2.25	4.59	8.3	2.20	4.62	2.21
	291.2	2.24			2.18	4.25	
	297.2	2.19			2.15	3.88	
	303.2	2.21			2.13	3.51	
	315.2	1.99			2.08	2.78	
13DMB	285.2	2.23	5.16	10	2.19	3.84	2.31
	291.2	2.21			2.17	3.43	
	297.2	2.12			2.14	3.03	
	303.2	2.13			2.12	2.62	
	315.2	1.92			2.07	1.81	
14DMB	285.2	2.23	4.65	8.6	2.19	3.82	2.49
	291.2	2.18			2.17	3.38	
	297.2	2.13			2.14	2.93	
	303.2	2.13			2.12	2.49	
	315.2	1.95			2.07	1.60	
135TMB	285.2	2.46	5.62	11	2.56	3.98	2.56
	291.2	2.48			2.53	3.52	
	297.2	2.42			2.49	3.06	
	303.2	2.26			2.46	2.61	

[a] Determined from linear interpolation of temperature-dependent free energy. [b] Values derived from eq 18. [c] Values derived from data set of Ashworth and co-workers.[29] [d] B indicates benzene.

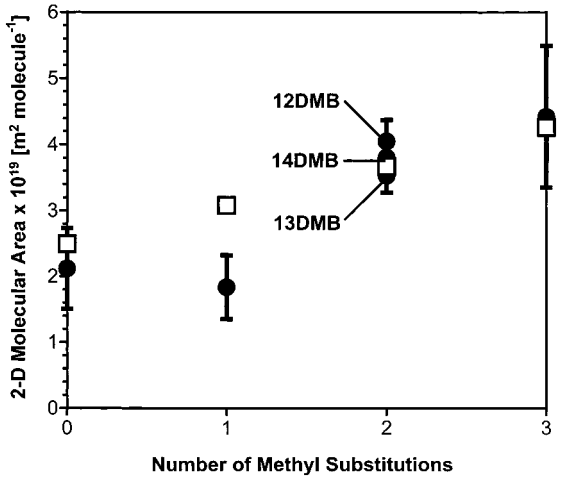

Figure 7. Ideal standard molar Gibbs free energy change of adsorption $\Delta_{ads}g^{0,ideal}_{(V\rightarrow I)}$ as a function of temperature T for benzene (open circle), MB (upright triangle), 12DMB (solid square), 13DMB (square with "×" inside), 14DMB (open square), and 135TMB (upside down triangle). Lines represent linear interpolation of the composite solute data (symbols): dashed line, 13DMB interpolation; dotted line, 14DMB interpolation. Error bars represent the maximum difference between values calculated from combined replicate isotherms (symbols) and individual replicates. Benzene (dotted circle), MB (solid upside down triangle), and 12DMB ("×") from Blank and Ottewill;[23] MB (solid upright triangle) from Hauxwell and Ottewill.[24]

where

$$\Delta_{henry}g^{0,ideal}_{(V\rightarrow W)} = -RT\ln[K_h] \qquad (18)$$

$\Delta_{henry}g^{0,ideal}_{(V\rightarrow W)}$ is the free energy change of transfer of a solute from the vapor-phase to the aqueous-phase (i.e., $V\rightarrow W$) [J mol^{-1}], K_h is the Henry's law partitioning coefficient [m^3_V m$^{-3}_W$], A_m is the three-dimensional molar surface area (van der Waals) [m^2 mol^{-1}], ϕ is the water/solute interaction parameter [unitless], σ_{IV} is the pure solute surface tension [N m^{-1}], and σ_{WV} is surface tension of solute-free water [N m^{-1}]. (Temperature-dependent K_h values from Ashworth and co-workers;[29] A_m, σ_{IV}, and σ_{WV} from Daubert and Danner;[30] and ϕ from Girifalco and Good.[31]) The provided form of the Valsaraj model assumes a molecular orientation where three-quarters of the solute area is in contact with the aqueous phase. Results of this approach and comparison to the current composite data indicate agreement within 10% over the temperature range considered (Table 2). The model predicts a smaller change in free energy as a function temperature than described by our data; however, the quantitative link between VHOC molecular size and adsorption energetics and the close prediction of our current results is of significant regard.

Ideal Enthalpy Change. Ideal standard molar enthalpy changes of adsorption, indicative of the strength of interaction between solute and interface water molecules, were calculated from linear interpolations to the composite ideal molar free energy change of adsorption versus temperature results for each solute. Values (symbols) are illustrated in Figure 8 as a function of number of methyl substitutions; error bars represent the maximum difference between combined and individual replicate results. In general, the VHOC enthalpy changes derived from the composite replicate experiments become more negative with increasing number of methyl substitutions, indicative of additive dispersion-type intermolecular forces. Assuming a linear fit to the data, an approximate increase in the exothermic enthalpy change of adsorption of 3.3×10^3 J mol^{-1} is

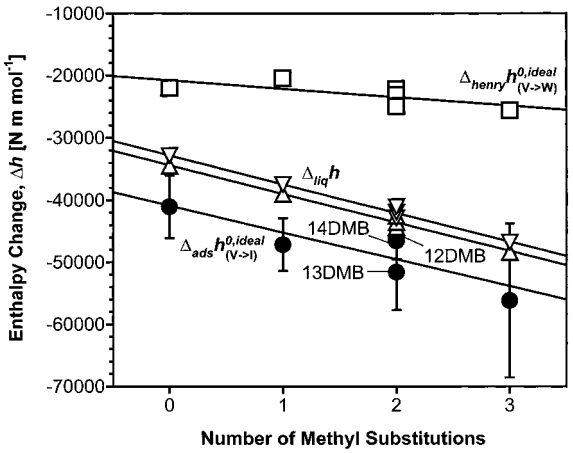

Figure 8. Ideal standard molar enthalpy change of adsorption $\Delta_{ads} h^{0,ideal}_{(V\rightarrow I)}$ as a function of number of methyl substitutions (solid circle) (error bars represent the maximum difference between values calculated from combined replicate isotherms (symbols) and individual replicates); enthalpy change of vapor/water transfer, $\Delta_{henry}h^{0,ideal}_{(V\rightarrow W)}$ (square);[29] enthalpy change of liquefaction $\Delta_{liq}h$ at 285.2 K (upright triangle) and 315.2 K (upside down triangle).[30] Lines represent linear interpolation of the corresponding absolute data.

derived for each additional methyl group added to the benzene ring.

Comparison of our composite calculated ideal adsorption enthalpy changes to the corresponding heats of liquefaction $\Delta_{liq}h$ at 285.2 and 315.2 K suggests that the adsorption is a more exothermic process (as much as 9.6×10^3 J mol^{-1} more negative) than the corresponding condensation of pure solute and that the trends as a function methyl substitution appear parallel (Figure 8). Additionally, with the exception of benzene, the composite values are also more negative than the heat of liquefaction for water (-4.39×10^4 J mol^{-1} at 297.2 K).[30] Further comparison to the enthalpy changes of transfer of the solutes from the vapor phase to the aqueous phase $\Delta_{henry}h^{0,ideal}_{(v\rightarrow w)}$ suggests a significantly more exothermic process ($\sim 2-3 \times 10^4$ J mol^{-1}) for interface VHOC adsorption (Table 2, Figure 8).

The presented relationships between ideal adsorption enthalpy changes to the other related phase transfer enthalpy changes indicate that the interaction fields between interfacial water molecules and adsorbed solutes are markedly different than between water and solutes in dilute aqueous solution and between solutes in bulk organic liquid. It has been reported by several researchers that benzene rings engage in hydrogen bonding with surrounding water molecules, possibly contributing to the strength and specificity of the bonding arrangement beyond condensed solute.[32−34] The same studies also indicate that the interactions are a function of number and orientation of surrounding water molecules. In light of our current results and these past studies, it might be suggested that the differences between enthalpy changes on adsorption at the vapor/water interface and for transfer of the solutes to the aqueous phase may be partly the result of different water−solute orientations. However, without more definitive understanding of the structure of the vapor/vapor interface, and the associations between adsorbed solutes and interface-phase water molecules, the exact mechanisms of adsorption and interaction are still unclear.

Ideal Entropy Change. Ideal standard molar entropy changes of adsorption were calculated using the linear interpolation to the composite ideal free energy changes of adsorption versus temperature results. Results are presented in Table 2 (with estimated errors from individual replicate calculations of ~20% for benzene, MB, DMB, and ~40% for 135TMB). All values indicate a decrease in entropy on solute adsorption, with an approximate 9 J mol^{-1} K^{-1} greater entropy loss per methyl addition; however, possible differentiation of the values as a function methyl-substitution was not possible due to high relative errors. Results are compared to the calculated loss of one degree of translational freedom, derived from the difference between the three-dimensional translational molar entropy ($_3s_{trans}$) [J mol^{-1} K^{-1}] of a gas at 1 atm, given by the Sackur−Tetrode equation as

$$_3s_{trans} = R\ln(M^{3/2}T^{5/2}) - 9.63 \qquad (19)$$

where M is the molecular mass [g mol^{-1}], and the translational molar entropy expression for a two-dimensional gas defined by Kemball is[35]

$$_2s_{trans} = R\ln(10^4 MTa/N_A) + 275.5 \qquad (20)$$

where a is the molar area defined in the standard state as $1.368 \times 10^5 T$ [m^2 mol^{-1}] and N_A is the Avogadro constant. Calculations using eqs 19 and 20 for the solutes and temperatures considered give translational entropy losses between -3.7×10^1 and -3.9×10^1 J mol^{-1} K^{-1}. It is apparent that this model does not define the same entropy loss of adsorption as calculated from isotherm measurement, suggesting further mechanisms of solute interaction and restriction (e.g., vibration, rotational) at the vapor/water interface.[26,35,36]

Conclusions

The reported vapor-phase dynamic adsorption method incorporating axisymmetric drop shape analysis-profile (ADSA-P) and gas chromatographic analysis provides a robust and accurate method for determining adsorption of volatile hydrophobic organic compounds (VHOCs) at the vapor/water interface. Results from this study further the understanding that there is a strong link between adsorption of relatively nonpolar, nonionic molecules at the vapor/water interface, and the corresponding molecular size. Furthermore, the calculated energetics of ideal adsorption, supported by the high measurement resolution at low vapor-phase VHOC pressures and the good internal consistency of the data, suggest that adsorption at the interface is accompanied by specific solute−water interactions. Further measurements of other compound suites are necessary to confirm this interpretation.

Acknowledgment. The project described was supported by grant number 2 P42 ESO4940-11 from the National Institute of Environmental Health Sciences, NIH with funds from U.S. EPA. Its contents are solely the responsibility of the authors and do not necessarily represent the official views of the NIEHS, NIH. The authors are extremely appreciative of comments and suggestions provided by Mr. Timothy Corley (University of Arizona), Dr. James Farrell (University of Arizona), Dr. Ingrid Padilla (Gregory L. Morris & Assoc.), Dr. Srini Raghavan (University of Arizona), and Mr. Jeffery Silva (Duke Engineering & Services), and the reviewers of this manuscript.

References and Notes

(1) Conklin, M. H.; Corley, T. L.; Roberts, P. A.; Davis, J. H.; van de Water, J. G. *Water Resour. Res.* **1995**, *31*, 1355.
(2) Gustafsson, Ö.; Gschwend, P. M. *Atmos. Environ.* **1999**, *33*, 163.
(3) Hoff, J. T.; Mackay, D.; Gillham, R.; Shiu, W. Y. *Environ. Sci. Technol.* **1993**, *27*, 2174.
(4) Hoff, J. T.; Gillham, R.; Mackay, D.; Shiu, W. Y. *Environ. Sci. Technol.* **1993**, *27*, 2789.

(5) Pennell, K. D.; Rhue, R. D.; Rao, P. S. C.; Johnston, C. T. *Environ. Sci. Technol.* **1992**, *26*, 756.
(6) Valsaraj, K. T. *Water Res.* **1994**, *28*, 819.
(7) Cheng, P.; Li, D.; Boruvka, L.; Rotenberg, Y.; Neumann, A. W. *Colloids Surf.* **1990**, *43*, 151.
(8) Cheng, P.; Neumann, A. W. *Colloids Surf.* **1992**, *62*, 297.
(9) Bruant, R. G., Jr.; Conklin, M. H. *J. Phys. Chem. B* **2000**, *104*, 11146.
(10) Bruant, R. G., Jr.; Conklin, M. H. *Environ. Sci. Technol.* **2001**. In press.
(11) Chattoraj, D. K.; Birdi, K. S. *Adsorption and the Gibbs Surface Excess*; Plenum: New York, 1984.
(12) Denbigh, K. *The Principles of Chemical Equilibrium*; Cambridge University Press: Cambridge, 1971.
(13) Prausnitz, J. M.; Lichtenthaler, R. N.; Gomes de Azevedo, E. *Molecular Thermodynamics of Fluid-Phase Equilibria*, 3rd ed.; Prentice Hall: Upper Saddle River, NJ, 1999.
(14) Smith, J. M.; Van Ness, H. C. *Introduction to Chemical Engineering Thermodynamics*, 4th ed.; McGraw-Hill: New York, 1987.
(15) Donaldson, D. J. *J. Phys. Chem. A* **1999**, *103*, 62.
(16) Donaldson, D. J.; Anderson, D. *J. Phys. Chem. A* **1999**, *103*, 871.
(17) Kemball, C.; Rideal, E. K. *Proc. R. Soc. London* **1946**, *A187*, 53.
(18) Atkins, P. *Physical Chemistry*, 6th ed.; W. H. Freeman and Co.: New York, 1998.
(19) Adamson, A. W.; Gast, A. P. *Physical Chemistry of Surfaces*, 6th ed.; John Wiley and Sons: New York, 1997.
(20) Jones, D. C.; Ottewill, R. H. *J. Chem. Soc.* **1955**, 4067.
(21) Aveyard, R. Adsorption at the Air/Liquid, Liquid/Liquid, and Solid/Liquid Interfaces. In *Surfactants*; Tadros, Th. F., Ed.; Academic Press: London, 1984.
(22) Volmer, M. *Z. Phys. Chem.* **1925**, *115*, 263.
(23) Blank, M.; Ottewill, R. H. *J. Phys. Chem.* **1964**, *68*, 2206.
(24) Hauxwell, F.; Ottewill, R. H. *J. Colloid Interface Sci.* **1968**, *28*, 514.
(25) Hartkopf, A.; Karger, B. L. *Acc. Chem. Res.* **1973**, *6*, 209.
(26) Karger, B. L.; Castells, R. C.; Sewell, P. A.; Hartkopf, A. *J. Phys. Chem.* **1971**, *75*, 3870.
(27) Karger, B. L.; Sewell, P. A.; Castells, R. C.; Hartkopf, A. *J. Colloid Interface Sci.* **1971**, *35*, 328.
(28) Valsaraj, K. T. *Chemosphere* **1988**, *17*, 875.
(29) Ashworth, R. A.; Howe, G. B.; Mullins, M. E.; Rogers, T. N. *J. Hazard. Mater.* **1988**, *18*, 25.
(30) Daubert, T. E.; Danner, R. P. *Physical and Thermodynamic Properties of Pure Chemicals: Data Compilation*; Hemisphere Publishing Co.: New York, 1989.
(31) Girifalco, L. A.; Good, R. J. *J. Phys. Chem.* **1957**, *61*, 904.
(32) Garrett, A. W.; Zwier, T. S. *J. Chem. Phys.* **1992**, *96*, 3402.
(33) Gotch, A. J.; Zwier, T. S. *J. Chem. Phys.* **1992**, *96*, 3388.
(34) Suzuki, S.; Green, P. G.; Bumgarner, R. E.; Dasgupta, S.; Goddard, W. A., III; Blake, G. A. *Science* **1992**, *257*, 942.
(35) Kemball, C. *Proc. R. Soc. London* **1946**, *A187*, 73.
(36) Davies, J. T.; Rideal, E. K. *Interfacial Phenomena*; Academic Press: New York, 1963.